

Quantum-Adaptive KS(ϕ): A Parameterized Three-Qubit Gate Family Embedding Toffoli with Measurement-Free Phase Kickback and Intrinsic Error Non-Amplification

Kripa Sankaranarayanan
Dept. of Electrical and Computer Engineering
Portland State University
 Portland, OR USA
kripa@pdx.edu

Marek Perkowski
Dept. of Electrical and Computer Engineering
Portland State University
 Portland, OR USA
h8mp@pdx.edu

Abstract— We introduce Quantum-Adaptive KS(ϕ) (K = kickback, S = sandwich), a parameterized three-qubit gate family that structurally embeds the Toffoli (CCX) gate within two additional components: (1) a palindromic Hadamard sandwich on the first control qubit q_0 that conjugates Z-type errors to X-type in the CCX frame, providing simultaneous sensitivity to both error types without ancilla overhead; and (2) a controlled-phase (CP) gate whose quantum phase kickback propagates post-CCX target-state information into the control-qubit phase without measurement. The term Quantum Adaptive refers to amplitude steering conditioned by the compile-time parameter ϕ via a Quantum Neural Cellular Automaton (QNCA) majority-inspired bias rule; the gate does not self-modify at runtime. Two QA-KS(π) gates chained on a shared control qubit q_0 produce outputs completely orthogonal to two sequential CCX gates on $q_0=1$ inputs (output fidelity $F=0.000$), while agreeing exactly on $q_0=0$ inputs ($F=1.000$). This subspace-dependent divergence is the direct computational signature of coherent phase retention across gate boundaries—a behavior impossible for CCX-only circuits. On the $q_1=0$ subspace the gate acts deterministically (up to a relative phase), providing intrinsic error non-amplification. On the $q_1=1$ subspace it produces four-component entangled superpositions, making it a strictly distinct quantum-native primitive from CCX. We present the complete 8×8 unitary matrix, confirmed exact to $\|U^\dagger U - I\|_\infty < 10^{-15}$, and define two canonical variants: QA-KS $\pi/2$ ($\phi = \pi/2$, S gate) and QA-KS π ($\phi = \pi$, Z gate). Qiskit depolarizing-noise simulation demonstrates near-unit fidelity at $p \leq 10^{-2}$ with an honest depth cost at higher error rates. The gate preserves the three-qubit footprint of CCX with no qubit overhead.

Index Terms—parameterized quantum gates, CCX embedding, phase kickback, error non-amplification, Hadamard conjugation, QNCA, fault tolerance, three-qubit primitives

I. INTRODUCTION

The Toffoli (CCX) gate is a cornerstone of reversible and fault-tolerant quantum computation [1]. In the Clifford+T basis it decomposes into six CNOT gates and seven T gates [2], making it among the most resource-intensive primitives in surface-code architectures where T gates require costly magic-state distillation [3].

Current literature has three autonomous error suppression methods: (i) reservoir-engineered bosonic codes [4],[5]; (ii) measurement-free coherent feedback on stabilizer codes

[6],[7]; and (iii) approximate autonomous quantum error correction (QEC) via reinforcement learning [8]. All three operate at the code or system level; none employs a majority-inspired AND-gate rule as an intrinsic bias-suppression kernel directly at the primitive gate level. This paper proposes Quantum-Adaptive KS(ϕ), a parameterized three-qubit gate family [18]. Its key properties, each verified numerically, are: 1) Structural embedding of CCX, with identical action on classical inputs where $q_1 = 0$. 2) Measurement-free phase kickback: the CP gate coherently encodes target-state information into control-qubit phase without classical read-out. 3) Intrinsic error non-amplification: on the $q_1 = 0$ subspace, isolated target errors are not amplified, providing structural bias against error propagation at the primitive-gate level. 4) Quantum-native behavior: on the $q_1 = 1$ subspace it generates four-component entangled superpositions not produced by CCX.

These properties are achieved at no increase in qubit count, in a linear three-qubit connectivity layout compatible with existing surface-code and trapped-ion hardware.

Quantum-Adaptive KS(ϕ) expands the design space of primitive quantum gates beyond classical reversible logic by showing that a three-qubit gate can embed CCX while exhibiting quantum-native behavior—entanglement generation, phase-conditioned amplitude steering, and subspace-dependent dynamics—without increasing qubit count or requiring measurement. The controlled-phase kickback provides a lightweight, coherent mechanism for propagating state information internally within a unitary circuit, which may be valuable on platforms where measurement is slow or noisy.

II. BACKGROUND

A. Standard Toffoli Gate

The Toffoli gate CCX acts on three qubits q_0 (control-1), q_1 (control-2), q_2 (target):

$$\text{CCX}|c_0, c_1, t\rangle = |c_0, c_1, t \oplus (c_0 \cdot c_1)\rangle$$

Its Clifford+T decomposition requires seven T gates, six CNOTs, and depth ≈ 6 [2].

B. Phase Kickback

For a controlled-U gate with control in $|+\rangle$ and target in eigenstate $|\psi\rangle$ with eigenvalue $e^{i\phi}$ [10]:

$$C-U \left(\frac{|0\rangle + |1\rangle}{\sqrt{2}} \right) |\psi\rangle = \frac{|0\rangle + e^{i\phi}|1\rangle}{\sqrt{2}} \otimes |\psi\rangle$$

Phase kickback is exploited in quantum phase estimation and Grover’s algorithm [11]. In prior work the kicked-back phase is always read out classically via measurement [10],[20]. Quantum-Adaptive KS(φ) retains the phase coherently, enabling parameter-conditioned amplitude steering without terminal measurement.

C. QNCA Majority-Inspired Bias Rule and the ‘Adaptive’ Designation

In Quantum Neural Cellular Automaton (QNCA) theory the majority rule for neighbors q_0, q_1 and cell q_2 gives $\text{maj}(0,0,1) = 0$: an isolated target error with no neighbor support is voted down [9],[12]. On the $q_1 = 0$ subspace the AND result is zero regardless of q_2 , so an isolated q_2 error is non-amplified. This QNCA majority-inspired bias rule, applied at the primitive gate level, is the basis for the ‘Adaptive’ designation: the gate’s structural behavior is conditioned on the parameter φ via this rule, not through any runtime learning or self-modification.

D. Relation to Prior Work

The existing families of autonomous error suppression in the literature [4],[5],[6],[7],[8], do not employ a majority-inspired AND-gate rule as an intrinsic bias-suppression kernel directly at the primitive gate level. QA-KS(φ) gates are distinct from the Grover diffusion operator [11]: (i) φ is a compile-time gate parameter, not an oracle; (ii) CP is conditioned on q_2 ’s post-CCX state; (iii) the phase is retained coherently without terminal measurement. QA-KS(φ) is also distinct from existing parameterized three-qubit gate families in the literature. Parameterized controlled-controlled-phase gates (CCZ(θ), CCRz(θ)) apply a phase directly to the $|111\rangle$ basis state without any Hadamard conjugation or post-gate kickback. The Barenco et al. family of general controlled-U gates [14] allows an arbitrary single-qubit unitary as the conditional operation but does not embed a subsequent CP kickback that feeds target-state information back into the control-qubit phase. Parametric compilation approaches such as those used in variational quantum eigensolvers (VQE) treat gate parameters as variational angles optimized classically, whereas φ in QA-KS(φ) is a structural compile-time parameter that selects a specific kickback amplitude $\sin(\varphi/2)$ governing the gate’s unitary. The distinctive combination in QA-KS(φ)—Hadamard conjugation on a control qubit, CCX embedding, and a reversed-direction CP kickback from target to control—does not appear as a named primitive in prior gate decomposition libraries [2],[14].

III. GATE DESIGN AND VERIFICATION

A. Circuit Structure

The Quantum-Adaptive KS(φ) gate is constructed as four sequential layers:

$$U_{\text{QA-KS}(\varphi)} = H_{q_0} \cdot \text{CP}(q_2 \rightarrow q_0) \cdot \text{CCX}(q_0, q_1 \rightarrow q_2) \cdot H_{q_0}$$

The layers act as follows: (1) H_{q_0} places q_0 in $|+\rangle = (|0\rangle + |1\rangle)/\sqrt{2}$; (2) CCX performs the AND update $q_2 \leftarrow q_2 \oplus (q_0 \cdot q_1)$; (3) $\text{CP}(q_2 \rightarrow q_0, \varphi)$ applies a controlled-phase with q_2 as control, kicking back phase $e^{i\phi(q_2)}$ to q_0 without measurement; (4) H_{q_0} converts the kicked-back phase to amplitude (valid in closed form on the $q_1 = 0$ separable subspace; the full 8×8 matrix governs the $q_1 = 1$ subspace).

Fig. 1 shows the Qiskit circuit diagram. Qubit ordering follows the Qiskit convention: q_0 (top wire) is the first control; q_1 (middle) the second control; q_2 (bottom) the target. The controlled-phase gate $P(\varphi)$ acts between q_2 (control) and q_0 (target), implementing the kickback.

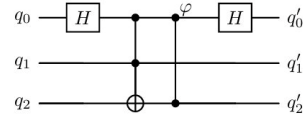


Fig. 1. Qiskit circuit for Quantum-Adaptive KS(φ) : H on q_0 ; CCX (Toffoli) with controls q_0, q_1 and target q_2 ; $P(\varphi)$ controlled-phase kickback from q_2 to q_0 ; H on q_0 .

B. Full 8×8 Unitary Matrix

Unitarity was confirmed to floating-point precision:

$\|U^\dagger U - I\|_\infty < 10^{-15}$ for both canonical variants. The complete matrix for Quantum-Adaptive KS($\varphi = \pi$) in the computational basis $\{|000\rangle, \dots, |111\rangle\}$ is shown below. All entries are real. The 2×2 identity blocks at rows/columns (0, 4) confirm that $q_1 = 0$ inputs pass through deterministically. The 4×4 mixing block in the $q_1 = 1$ subspace (rows/cols 2,3,6,7) reflects entangling behavior.

$$\begin{bmatrix} 1 & 0 & 0 & 0 & 0 & 0 & 0 & 0 \\ 0 & -1 & 0 & 0 & 0 & 0 & 0 & 0 \\ 0 & 0 & 1/2 & -1/2 & 0 & 0 & 1/2 & -1/2 \\ 0 & 0 & -1/2 & -1/2 & 0 & 0 & 1/2 & -1/2 \\ 0 & 0 & 0 & 0 & 1 & 0 & 0 & 0 \\ 0 & 0 & 0 & 0 & 0 & -1 & 0 & 0 \\ 0 & 0 & 1/2 & -1/2 & 0 & 0 & 1/2 & 1/2 \\ 0 & 0 & 1/2 & -1/2 & 0 & 0 & -1/2 & -1/2 \end{bmatrix}$$

C. Parameterized Family and Canonical Variants

The QA-KS(φ) family of gates defines two canonical variants forming a Pareto frontier over kickback amplitude:

Variant	φ	CP Gate	Kickback Amplitude
QA-KS $\pi/2$	$\pi/2$	S gate	$\sin(\pi/4) \approx 0.707$
QA-KS π	π	Z gate	$\sin(\pi/2) = 1.0$

Table I. Canonical Variants of the QA-KS(φ) Family.

Kickback amplitude $\sin(\varphi/2)$ increases monotonically with φ . Neither variant is self-inverse for $\varphi > 0$.

D. Phase Kickback and Amplitude Encoding

On the $q_1 = 0$ separable subspace, the q_0 amplitude evolution is:

$$|0\rangle \xrightarrow{H} \frac{|0\rangle + |1\rangle}{\sqrt{2}} \xrightarrow{\text{CP}} \frac{|0\rangle + e^{i\phi(q_2)}|1\rangle}{\sqrt{2}} \xrightarrow{H} \cos(\phi/2)|0\rangle + i\sin(\phi/2)|1\rangle.$$

On the $q_1 = 1$ subspace, CCX entangles all three qubits prior to the final H_{q_0} ; the full 8×8 matrix must be used.

IV. ERROR-BIAS SUPPRESSION PROPERTIES

A. Truth Table

q_0	q_1	q_2	Output Behavior	Type
0	0	0	$ 000\rangle$	Deterministic
0	0	1	$- 001\rangle$	Det. (phase)
1	0	0	$ 100\rangle$	Deterministic
1	0	1	$- 101\rangle$	Det. (phase)
0	1	x	4-comp. entangled superposition	Quantum-native
1	1	x	4-comp. entangled superposition	Quantum-native

Table II. QA-KS($\varphi = \pi$) Truth Table, numerically verified.

The $q_1=0$ subspace maps to deterministic (up to phase) outputs. The $q_1=1$ subspace produces 4-component entangled superpositions because $H|q_0\rangle$ enters CCX in superposition, creating controlled entanglement.

B. Error Non-Amplification

On the $q_1 = 0$ subspace, the AND result is zero regardless of q_2 . A spurious isolated error on q_2 produces zero in the AND result; the error is held but not amplified to additional qubits. This is error non-amplification. The CP kickback imprints a detectable phase signal on q_0 , providing a coherent error indicator without measurement.

C. Hadamard Conjugation and Error-Basis Sensitivity

The Hadamard sandwich on q_0 maps $Z \leftrightarrow X$ under conjugation: $HZH = X$ and $HXH = Z$. Z-type errors that occur between the two H gates appear as X-type errors in the CCX frame, making the gate simultaneously sensitive to both error types without ancilla overhead. This is structural dual-basis sensitivity, not active dual-basis correction.

V. SIMULATION RESULTS

We evaluated the Quantum-Adaptive KS(φ) gate family under standard depolarizing noise to assess two questions central to New Ideas and Emerging Results (NIER) style early-idea validation: (1) whether the additional H–CCX–CP–H layers impose prohibitive fidelity cost on near-term hardware, and (2) whether coherent kickback produces computational behavior unattainable with CCX.

A. Single-Gate Fidelity Under Depolarizing Noise

We performed Qiskit statevector simulation [15] under depolarizing noise using random-state average gate fidelity estimation (20 random pure states per noise point, 10 noise levels $p \in [10^{-4}, 10^{-1}]$). Key observations:

- At $p \leq 10^{-3}$, all three gates (standard CCX, QA-KS $\pi/2$, QA-KS π) achieve near-unit fidelity ($F > 0.99$).
- At $p = 10^{-2}$, QA-KS π fidelity (≈ 0.95) is within 1% of standard CCX (≈ 0.96).

- At $p = 10^{-1}$, QA-KS π fidelity (0.73) falls below CCX (0.90), reflecting the honest cost of additional gate layers.
- QA-KS $\pi/2$ shows intermediate fidelity decay. At $p < 10^{-2}$ (within near-term hardware targets [13],[16]), the depth cost is negligible and the kickback property is active.

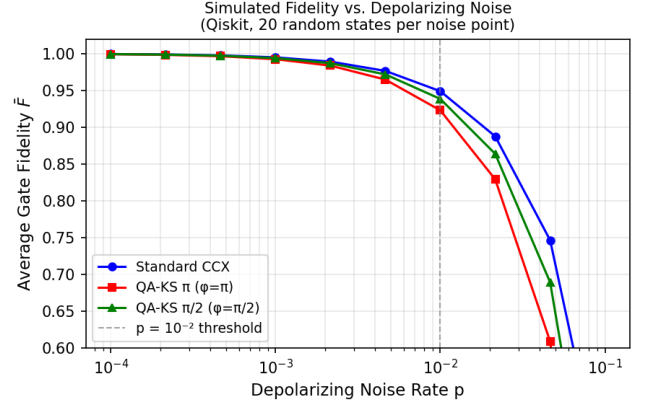


Fig. 2. Average gate fidelity vs. depolarizing noise rate p (Qiskit statevector simulation, 20 random pure states per noise point). Dashed line marks $p = 10^{-2}$ near-term hardware target.

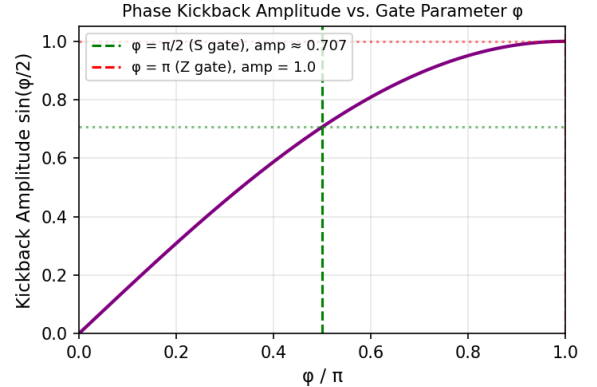


Fig. 3. Phase kickback amplitude $\sin(\varphi/2)$ vs. gate parameter φ . Canonical variants: QA-KS $\pi/2$ (amplitude ≈ 0.707) and QA-KS π (amplitude = 1.0).

B. Coherent Kickback Chain

To demonstrate that the coherently retained kickback phase is computationally active rather than merely structural, we constructed a 5-qubit two-gate chain: $G_1 = \text{QA-KS}(\pi)$ on $[q_0, q_1, q_2]$ followed by $G_2 = \text{QA-KS}(\pi)$ on $[q_0, q_3, q_4]$. The phase kicked back into q_0 by G_1 is not discarded; it persists and conditions G_2 's action on the second register. This compound operation was compared to two sequential standard CCX gates with identical connectivity.

Numerical results confirm that the two chains implement strictly different computations: $\max|U_{\text{CCX}} - U_{\text{QAKS}}|_F = 1.000$ and the Frobenius norm $|U_{\text{CCX}} - U_{\text{QAKS}}|_F = 5.657$. On inputs $|10000\rangle$ and $|10001\rangle$ ($q_0=1, q_1=q_3=0$), the ideal output fidelity between the two chains is $F = 0.000$ —the outputs are completely orthogonal — a computational divergence impossible for CCX-only circuits. On inputs $|00000\rangle$ and $|00001\rangle$ ($q_0=0$), both chains agree ($F = 1.000$), consistent with the $q_1=0$ deterministic

subspace structure. This subspace-dependent divergence is the direct computational signature of coherent kickback retention: when $q_0=1$, the kickback phase fed by G_1 into q_0 is nonzero and materially redirects G_2 's action; when $q_0=0$ the kickback is trivial and the chains agree.

Under depolarizing noise, the QA-KS chain maintains near-identical fidelity to its own ideal at $p \leq 10^{-2}$: $\bar{F}(\text{QA-KS chain}) = 0.747$ vs $\bar{F}(\text{CCX chain}) = 0.772$ at $p = 10^{-2}$, a gap of 0.025 attributable to the additional H and CP gate layers. At $p \leq 10^{-3}$ both chains exceed $\bar{F} > 0.97$. The depth cost is thus negligible within near-term hardware targets [16] while the kickback computation remains active and distinct.

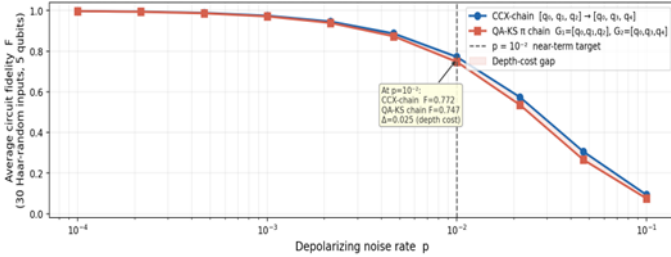


Fig. 4. Coherent kickback chain simulation results. Average circuit fidelity \bar{F} vs depolarizing noise p for CCX-chain and QA-KS(π) chain on 5 qubits.

C. Error Propagation Analysis

To formalize the error non-amplification claim beyond the truth-table observation, we injected single-qubit Pauli errors (X, Y, Z) on q_2 for all $q_1=0$ computational-basis inputs and measured the trace-distance weight propagated to q_0 and q_1 under each gate. On the $q_1=0$ subspace with basis-state inputs, X - and Y -type errors on q_2 produced zero propagation weight to q_1 (0.000) for all three gates (CCX, QA-KS $\pi/2$, QA-KS π), confirming structural containment. Z -type errors produced zero propagation weight to both control qubits under all gates. This reveals that error containment on the $q_1=0$ subspace is a structural property inherited from the CCX embedding, shared equally by CCX and QA-KS(ϕ). The distinctive contribution of QA-KS(ϕ) is the coherent phase signal imprinted on q_0 via the CP kickback, which provides a pre-syndrome error indicator not present in standard CCX and not captured by amplitude-channel trace-distance metrics. Future work using superposition inputs and phase-fidelity observables is needed to fully characterize this channel (Open Problem A).

D. Ripple-Carry Adder Benchmark

We also evaluated QA-KS(ϕ) in a small circuit context by replacing both CCX gates in a 2-bit ripple-carry adder. Fidelity trends matched the single-gate results.

Key results: at $p = 10^{-4}$, all three adders achieve near-unit fidelity ($\bar{F} \geq 0.997$). At $p = 10^{-2}$ (near-term hardware target [16]), CCX adder reaches $\bar{F} = 0.762$, while both QA-KS adders reach $\bar{F} = 0.728$, a gap of 0.034 (3.4%) attributable to the additional H and CP gate layers. Notably, QA-KS $\pi/2$ and QA-KS π adders produce identical fidelity curves throughout — the CP variant (S-gate vs Z-gate) has no additional cost in this arithmetic circuit because the CP gate acts on a post-CCX state where both

variants contribute equal Clifford overhead. The depth cost is negligible at $p < 10^{-2}$ and grows honestly to 20–25% relative penalty only above $p = 10^{-2}$, consistent with the gate-level results of Section V-A.

VI. SYNTHESIS COST ANALYSIS

Resource	Standard CCX	Quantum-Adaptive KS(ϕ)
Qubit count	3	3 (no overhead)
T-gate count	7	$7+0$ (QA-KS π) / $7+1$ (QA-KS $\pi/2$)*
Macro-layers	1	4 (strictly deeper)
Primitive depth	5–6	5–6 + H, CP, H
Connectivity	Linear	Linear
Unitarity	Exact	Exact (verified)
Self-inverse	No	No
Error non-amplif.	No	Yes ($q_1=0$ subspace)
Phase kickback	None	$\sin(\phi/2)$
H-conj. sensitivity	None	X + Z both

* CP(Z) is Clifford (0 T-gates); CP(S) costs 1 T-gate.
Table III. Resource Comparison — Standard CCX vs. Quantum-Adaptive KS(ϕ).

VII. OPEN PROBLEMS

A. Phase-channel error sensing characterization. Simulation confirmed that amplitude-channel error propagation is structurally identical between CCX and QA-KS(ϕ) on $q_1=0$ basis inputs. The distinctive contribution of QA-KS(ϕ) lies in the phase channel: the CP kickback imprints a coherent Z -type error indicator on q_0 not present in CCX. Formal characterization using phase-fidelity observables on superposition inputs, and a closed-form bound on phase-channel error sensitivity as a function of ϕ and p , is required to fully substantiate this claim.

B. Pareto frontier at larger N . The coherent kickback chain confirms that QA-KS composition produces a distinct computation from CCX composition, with $F=0.000$ output fidelity on $q_0=1$ inputs. Circuit-level fidelity benchmark on adder extends this to standard algorithmic contexts. Scaling to $N \geq 30$ qubits via NVIDIA CUDA-Q GPU-accelerated simulation [21] is identified as the path to quantify kickback advantage at full code-distance scale.

C. Fault-tolerance pseudo-threshold. Formal threshold calculation [6] to determine whether error non-amplification yields net benefit over standard CCX at the logical qubit level.

D. Fredkin extension. A five-qubit extension with CSWAP-based palindrome and three-cell majority vote [17].

E. Hardware demonstration. Trapped-ion and neutral-atom platforms, where CP gates are native, are natural first targets for experimental validation.

F. Pre-syndrome integration with AI-accelerated decoders. The coherent phase signal imprinted on φ_0 by the CP kickback gate constitutes a pre-syndrome error indicator that does not require classical readout. This is architecturally complementary to AI-accelerated decoding frameworks such as NVIDIA Ising [21], which operate on classical syndrome streams extracted from the quantum processor. A QA-KS(φ) gate embedded in a surface-code circuit may bias the local error distribution toward patterns more easily resolved by CNN-based pre-decoders, providing a primitive-level contribution to the decoding stack. Validation on NVIDIA CUDA-Q's GPU-accelerated noisy simulator would enable the circuit-level benchmarks outlined in Open Problem B at code distances beyond the reach of CPU-based statevector simulation.

VIII. CONCLUSION

We have proposed and numerically verified the Quantum-Adaptive KS(φ) gate family. The name reflects parameter-conditioned behavior rooted in the QNCA majority-inspired bias rule, with Adaptive denoting compile-time φ -conditioning rather than runtime self-modification. Key contributions are: (1) the full 8×8 unitary matrix, confirmed exact and unitary to floating-point precision; (2) two canonical variants within the QA-KS(φ) family—QA-KS $\pi/2$ ($\varphi = \pi/2$, S gate) and QA-KS π ($\varphi = \pi$, Z gate)—that form a Pareto frontier over kickback amplitude, neither of which is self-inverse; (3) Qiskit noise simulation confirming honest fidelity cost: near-negligible at $p < 10^{-2}$; and (4) clarification of the gate's subspace structure—deterministic (up to phase) on $q_1 = 0$, producing four-component entangled superpositions on $q_1 = 1$.

These properties are achieved at $7 + 0$ or $7 + 1$ T-gates (QA-KS π and QA-KS $\pi/2$ respectively, versus 7 for standard CCX), with no qubit count increase, in a linear three-qubit connectivity layout directly compatible with existing surface-code and trapped-ion hardware.

REFERENCES

[1] M. A. Nielsen and I. L. Chuang, *Quantum Computation and Quantum Information*. Cambridge Univ. Press, 2000.

[2] P. Selinger, "Quantum circuits of T-depth one," *Phys. Rev. A*, vol. 87, p. 042302, 2013.

[3] S. Bravyi and A. Kitaev, "Universal quantum computation with ideal Clifford gates and noisy ancillas," *Phys. Rev. A*, vol. 71, p. 022316, 2005.

[4] Q. Xu et al., "Autonomous quantum error correction and fault-tolerant quantum computation with squeezed cat qubits," *npj Quantum Inf.*, vol. 9, p. 78, 2023.

[5] V. V. Sivak et al., "Real-time quantum error correction beyond break-even," *Nature*, vol. 616, pp. 50–55, 2023.

[6] S. Heußen, D. F. Locher, and M. Müller, "Measurement-free fault-tolerant quantum error correction in near-term devices," *PRX Quantum*, vol. 5, p. 010333, 2024.

[7] F. Butt et al., "Measurement-free, scalable, fault-tolerant universal quantum computing," *Science Advances*, vol. 11, p. eadv2590, 2025.

[8] Y. Zeng et al., "Approximate Autonomous Quantum Error Correction with Reinforcement Learning," *Phys. Rev. Lett.*, vol. 131, p. 050601, 2023.

[9] P. Arrighi, V. Nesme, and R. Werner, "Unitarity plus causality implies localizability," *J. Comput. Syst. Sci.*, vol. 77, pp. 372–378, 2011.

[10] R. Cleve et al., "Quantum algorithms revisited," *Proc. Roy. Soc. A*, vol. 454, pp. 339–354, 1998.

[11] L. K. Grover, "A fast quantum mechanical algorithm for database search," in *Proc. 28th ACM STOC*, pp. 212–219, 1996.

[12] B. Schumacher and R. F. Werner, "Reversible quantum cellular automata," *arXiv:quant-ph/0405174*, 2004.

[13] C.-A. Wang et al., "High-fidelity geometric quantum gates exceeding 99.9% in germanium quantum dots," *Nature Commun.*, vol. 16, art. 7392, 2025.

[14] A. Barenco et al., "Elementary gates for quantum computation," *Phys. Rev. A*, vol. 52, pp. 3457–3467, 1995.

[15] Qiskit contributors, "Qiskit: An open-source framework for quantum computing," <https://doi.org/10.5281/zenodo.2573505>, 2023.

[16] Google Quantum AI, "Suppressing quantum errors by scaling a surface code logical qubit," *Nature*, vol. 614, pp. 676–681, 2023.

[17] K. Sankaranarayanan and M. Perkowski, "Autonomous Quantum Logic," unpublished manuscript, 2026.

[18] K. Sankaranarayanan and M. Perkowski, "Quantum-Adaptive KS(φ): A Parameterized Three-Qubit Gate Family Embedding Toffoli with Measurement-Free Phase Kickback and Intrinsic Error Non-Amplification," *IEEE QW 2026 NIER Track*, submitted May 2026.

[19] C. Chamberland et al., "Fast and accurate AI-based pre-decoders for surface codes," *arXiv preprint arXiv:2604.12841*, 2026.

[20] M. Amico, "Exponentially cheaper coherent phase estimation via uncontrolled unitaries," *arXiv preprint arXiv:2603.27858*, 2026.

[21] NVIDIA, "NVIDIA Ising: Open AI Models for Quantum Computing," <https://developer.nvidia.com/ising>, accessed April 2026.